



Estimation of Coda Wave Attenuation in Northern Morocco

ABDERRAHIM BOULANOUAR,^{1,2} LAHCEN EL MOUDNIB,² SIMANCHAL PADHY,³ MIMOUN HARNAFI,² ANTONIO VILLASEÑOR,⁴
JOSEP GALLART,⁴ ANTONIO PAZOS,⁵ ABDELAALI RAHMOUNI,¹ MOHAMED BOUKALOUCHE,¹ and JAMAL SEBBANI¹

Abstract—We studied the attenuation of coda waves and its frequency and lapse-time dependence in northern Morocco. We analysed coda waves of 66 earthquakes recorded in this region during 2008 for four lapse time windows of length 30, 40, 50, and 60 s, and at five frequency bands with central frequency in the range of 0.75–12 Hz. We determined the frequency dependent Q_c relation for the horizontal (NS and EW) and vertical (Z) component seismograms. We analyzed three-component broadband seismograms of 66 local earthquakes for determining coda-Q based on the single back-scattering model. The Q_c values show strong frequency dependence in 1.5–12 Hz that is related to high degree of heterogeneity of the medium. The lapse time dependence of Q_c shows that Q_0 (Q_c at 1 Hz) significantly increases with lapse time that is related to the depth dependence of attenuation and hence of the level of heterogeneity of the medium. The average frequency-dependent $Q_c(f)$ values are $Q_c = (143.75 \pm 1.09)f^{(0.864 \pm 0.006)}$, $Q_c = (149.12 \pm 1.08)f^{(0.85 \pm 0.005)}$ and $Q_c = (140.42 \pm 1.81)f^{(0.902 \pm 0.004)}$ for the vertical, north–south and east–west components of motion, respectively. The frequency-dependent $Q_c(f)$ relations are useful for evaluating source parameters (Singh et al. 2001), which are the key inputs for seismic hazard assessment of the region.

Key words: Attenuation, coda waves, northern morocco, Q_c , the single scattering model.

1. Introduction

Attenuation of high-frequency (> 1 Hz) seismic waves is one of the major components in evaluating the seismo-tectonic feature and seismic hazard assessment

of the region. The attenuation of seismic waves is expressed using the dimensionless quality factor Q , defined as the fractional loss of energy per unit cycle of the wave. One method for estimating coda-Q (Q_c) is from the decay rate of coda waves, waves scattered from randomly distributed heterogeneities of the medium (Mamdouh et al. 2013; Mukhopadhyay and Tyagi 2007; Kumar et al. 2005). The parameter Q_c represents the total attenuation properties of the earth's crust, that includes both intrinsic or anelastic absorption and scattering attenuation due to random heterogeneities of the medium (Lee 1999).

Numerous studies have been done worldwide to understand the attenuation characteristics of the medium using coda waves (Aki and Chouet 1975; Badawy and Morsy 2012; Boulanouar et al. 2013; Biescas et al. 2007; Giampiccolo et al. 2002; Gupta et al. 1998; Parvez et al. 2008; Sato et al. 2012). The results from these studies show that the values of Q_c vary with both frequency ($Q_c = Q_0 f^n$, Q_0 is the value of Q_c at 1 Hz (Singh and Hermann 1983) and n is frequency-dependent exponent) and lapse time. The lapse-time dependence of Q_c is attributed to the effect of both multiple scattering and depth (Masahiro 1992; Barros et al. 2011). The values of Q_c obtained with a single scattering model show that Q_0 is less (< 200) and n is high (≥ 1.0) for tectonically active regions, while Q_0 is more (> 200) and n is low (< 1) for stable areas (Sato et al. 2012).

Very little work has been done on seismic wave attenuation in northern Morocco, a region characterized by active subduction with complex tectonics (Boulanouar et al. 2013, 2016). Boulanouar et al. (2013) showed the spatial variation of coda wave attenuation using aftershocks of the Al Hoceima earthquake (MI = 6.4) of 24 February, 2004.

Here, we study the attenuation properties of the medium using coda waves beneath northern Morocco

¹ Physics Department, Faculty of Science, Mohamed V University, Rabat, Morocco. E-mail: aboulanouar1@gmail.com

² Earth Science Department, Scientific Institute, Mohamed V University, Rabat, Morocco.

³ National Geophysical Research Institute, Hyderabad 500007, India.

⁴ Institute of Earth Science “JaumeAlmera”, CSIC, Barcelona, Spain.

⁵ Geophysical Department, Royal Naval Observatory, San Fernando, Cadiz, Spain.

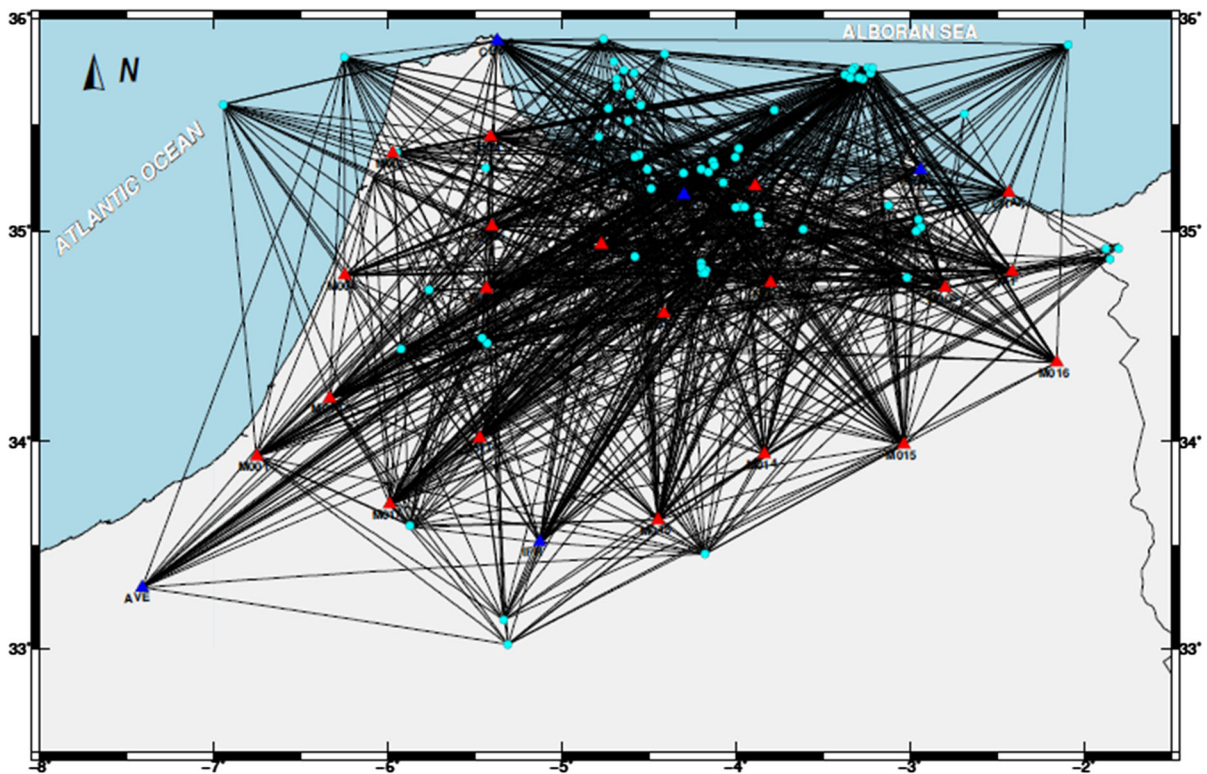


Figure 1

Map of the northern Morocco showing the ray traces used in this study (blue ones belongs to the western Mediterranean seismic network and the red ones to the IberArray network)

(Fig. 1), using the single back-scattering model of Aki and Chouet (1975) by analyzing a large number of three-component broad-band seismograms of local earthquakes during 2008. We also show dependence of Q_c on frequency and lapse-time, examine the Q_c estimates of three-components of motion, compare our results with those of other studies obtained with similar method, and finally correlate the results with the seismo-tectonic features of the region.

2. Data

The seismograms used in this study are from 66 local earthquakes (Table 1) recorded by 26 three-component broad-band stations (Table 2) equipped with Trillium 40 sensors (100 Hz). Figure 1 shows the map of the study area with the location of events and stations used in this study. The seismic stations are maintained by the Scientific Institute of Rabat.

The magnitudes of the analyzed events range from 0.7 to 3.4. The depth and epicentral distance of the events vary from 0 to 120.8 km, and from 12.4 to 289.0 km, respectively. Data were recorded digitally at 100 samples per second. Only good quality seismograms with signal-to-noise ratio greater than 3.0 were processed. The events used in this work (Fig. 1) are previously located using the (Instituto Geografico Nacional) (IGN) reference velocity model and selected from earthquake location database used in the local earthquake tomography of the Betic-Rif system, western Mediterranean (El Moudnib et al. 2015).

3. Method of Analysis

The coda decay rate of local earthquakes is found to be independent of source-receiver distance (Aki 1969). Assuming the single back-scattering model for coda generation for coincident source and receiver,

Table 1

List of earthquakes used for estimation of coda, Q

Origine time			Latitude (deg.)	Longitude (deg.)	Depth (km)	Magnitude (MI)
Date (dd/mm/yy)	Hr:Mn	Sec				
21/01/2008	02:24	0	35.118	- 3.977	5	0.8
25/01/2008	13:19	4	33.023	- 5.311	31.1	0
28/01/2008	16:09	25	35.021	- 2.936	6.4	1.9
11/02/2008	09:13	32	35.231	- 4.073	4.6	1.6
18/02/2008	15:10	32	34.47	- 5.431	6.2	3.5
19/02/2008	04:13	49	35.879	- 2.09	0	3.3
23/02/2008	15:43	17	35.581	- 4.733	8.7	3.1
01/03/2008	03:30	15	34.802	- 4.194	2.3	1
01/03/2008	03:53	55	34.817	- 4.174	0	1
01/03/2008	03:55	11	35.35	- 4.003	0	1
02/03/2008	02:07	44	34.442	- 5.926	0.4	1
12/03/2008	03:56	49	35.701	- 2.639	21.5	1
17/03/2008	16:05	39	35.572	- 3.78	6.8	1
24/03/2008	21:51	58	35.821	- 6.251	75	3
04/04/2008	01:14	0	35.362	- 4.556	86.2	2
09/04/2008	00:05	44	35.393	- 3.985	8.6	2
13/04/2008	11:06	39	35.01	- 3.614	9.1	2
14/04/2008	23:28	4	35.448	- 4.788	78.8	1
16/04/2008	01:09	18	35.115	- 4.001	5.8	2
27/04/2008	19:17	36	35.764	- 3.227	11.1	1
27/04/2008	19:30	59	35.773	- 3.241	9.7	1
28/04/2008	04:21	12	35.745	- 3.226	11	2
28/04/2008	11:23	49	35.771	- 3.214	17.8	2
29/04/2008	13:38	47	35.522	- 4.62	116.2	1
02/05/2008	21:41	17	35.761	- 3.333	0.1	1
03/05/2008	08:46	42	35.724	- 3.292	9.2	1
08/05/2008	16:57	33	35.907	- 4.762	112.7	2
09/05/2008	18:04	12	35.002	- 2.964	9.6	2
08/06/2008	00:59	34	34.781	- 3.017	5	2
13/06/2008	11:27	41	34.882	- 4.582	73.1	3
15/06/2008	08:26	13	32.428	- 4.824	59.9	2
28/06/2008	05:15	49	35.307	- 1.365	9.1	2
04/07/2008	15:41	6	35.331	- 4.132	8.4	1
04/07/2008	19:32	31	35.341	- 4.161	16.4	1
05/07/2008	00:43	16	35.313	- 4.124	6.5	1
05/07/2008	20:49	31	35.277	- 4.303	0	1
06/07/2008	17:00	46	35.296	- 4.201	6.9	1
19/07/2008	20:02	53	34.919	- 1.875	5	2
23/07/2008	13:41	28	35.595	- 4.547	105.6	1
26/07/2008	17:08	45	35.04	- 3.866	8.1	2
28/07/2008	02:16	35	35.76	- 4.645	106.7	2
03/08/2008	13:03	44	34.495	- 5.46	16.9	2
03/08/2008	19:04	46	34.883	- 1.855	10.1	1
04/08/2008	00:12	24	35.293	- 4.509	32	1
10/08/2008	21:10	28	34.92	- 1.801	3.2	1
08/08/2008	22:56	11	35.643	- 4.609	106.2	1
26/08/2008	02:10	6	35.203	- 4.488	22.4	1
26/08/2008	19:27	38	35.683	- 4.686	103.7	1
28/08/2008	03:59	59	34.802	- 4.179	5.4	2
29/08/2008	07:31	37	35.072	- 3.872	6.7	2
09/09/2008	13:36	40	35.598	- 6.948	77.8	4
11/09/2008	18:22	29	33.588	- 5.84	22.9	1
20/09/2008	20:09	28	35.836	- 4.411	120.8	2
23/09/2008	13:49	35	34.724	- 5.764	11.1	1

Table 1 *continued*

Origine time			Latitude (deg.)	Longitude (deg.)	Depth (km)	Magnitude (MI)
Date (dd/mm/yy)	Hr:Mn	Sec				
26/09/2008	10:19	55	35.252	− 6.082	68.6	2
28/09/2008	01:11	21	33.596	− 5.874	22.2	2
04/10/2008	17:47	55	35.116	− 3.951	11.2	2
04/10/2008	19:27	25	35.123	− 3.123	9.6	1
14/10/2008	18:59	24	34.869	− 1.85	0	1
01/11/2008	09:17	33	35.373	− 5.951	35	2
08/11/2008	21:16	58	33.142	− 5.335	12.4	0
12/11/2008	00:23	33	35.282	− 4.158	10.5	1
26/11/2008	02:45	56	35.72	− 4.688	85.3	1
27/11/2008	18:03	9	34.942	− 1.8	0	0
28/11/2008	23:34	27	35.352	− 4.581	87.9	1
23/12/2008	01:29	45	35.556	− 2.688	24.3	1

yy year, mm month, dd day, Hr hour, Mn minute, Sec second

Table 2

List of seismic stations that belong to the Morocco network

Station name	Station latitude (deg.)	Station longitude (deg.)
M001	33.929	− 6.756
M002	35.370	− 5.971
M004	34.791	− 6.249
M005	35.024	− 5.403
M006	34.938	− 4.775
M007	34.756	− 3.800
M008	34.732	− 2.797
M010	34.206	− 6.335
M011	34.016	− 5.472
M012	34.730	− 5.434
M013	34.610	− 4.414
M015	33.984	− 3.035
M016	34.378	− 2.156
M017	33.698	− 5.990
M019	31.937	− 4.456
M018	33.622	− 4.448
NKM	35.447	− 5.410
ALHU	35.213	− 3.890
CHAF	35.183	− 2.430
TAF	34.810	− 2.411
CEU	35.898	− 5.373
CEUT	35.53	− 5.196
MELI	35.289	− 2.939
PVLZ	35.173	− 4.301
ECEU	35.538	− 5.226
IFR	33.516	− 5.127

the amplitude of band-pass filtered coda envelope as a function of lapse time from origin time “ t ” can be expressed as (Aki and Chouet 1975):

$$A(f, t) = S(f) \times t^{-1} \exp\left(\frac{\pi ft}{Q_c}\right), \quad (1)$$

where $S(f)$ is the coda source factor at frequency f , Q_c is the quality factor for coda wave, t^{-1} accounts for the geometrical spreading for body waves. By taking the natural logarithms of Eq. (1) and rearranging terms, we obtain the following equation:

$$\ln[A(f, t) \times t] = C - b \times t, \quad (2)$$

where b and C equal to $-\pi f/Q_c$ and $\ln[S(f)]$, respectively. The Q_c values are calculated from the linear regression of $\ln[A(f, t) \times t]$ versus t for each frequency band centered at 0.75, 1.5, 3.0, 6.0 and 12.0 Hz (Table 3). Coda envelope can be obtained by taking the root mean squares (rms) of the signal in a sliding window. The linear regression was performed for four lapse time windows of 30–60 s starting from $2t_s$ (t_s is the S-wave arrival time) (Rautian and Khalturin 1978) to examine the lapse time dependence of Q_c . Finally, the power-law form of $Q_c = Q_0 f^n$ is fitted for the both the vertical and horizontal components for each station, where Q_0 is the Q_c -value at 1-Hz and n is the frequency relation parameter. Figure 2 shows an example of data processing used for determining Q_c at different frequency bands, using a vertical component seismogram from a representative event recorded at station CHAF.

4. Tectonic Setting

Northern Morocco belongs to the Iberia-Africa collision zone, which is one of the complex deformation zones in the western Mediterranean (Khattach et al.

Table 3

Parameters of a band-pass filter showing lower cut-off, higher cut-off and central frequencies

High cutoff (Hz)	Central frequency (Hz)	Low cutoff (Hz)
1	0.75	0.5
2	1.5	1
4	3	2
8	6	4
16	12	8

2013; Timoulali et al. 2014). The section beneath this collision zone is characterized by a diffuse and moderate seismicity, in comparison to the neighboring zones with large earthquakes in the east and the west (Cherkaoui and Hassani 2012; Inmaculada et al. 2003). The area under study experienced two moderate earthquakes in last decades (Boulanouar et al. 2016; Medina and Alami 2006) (Al Hoceima 2004, $M \sim 6.4$, Al Hoceima 1994, $M \sim 5.8$). The area is characterized by shallow (< 30 km) seismic activity that is concentrated in the Al Hoceima region and in the region immediate south to the Nador city. The annual frequency of the felt earthquakes (intensity $> V$) is 2.4 (Cherkaoui et al. 1990). The intermediate depth earthquakes occur in the region ranging from north-south to west of the Alboran Sea.

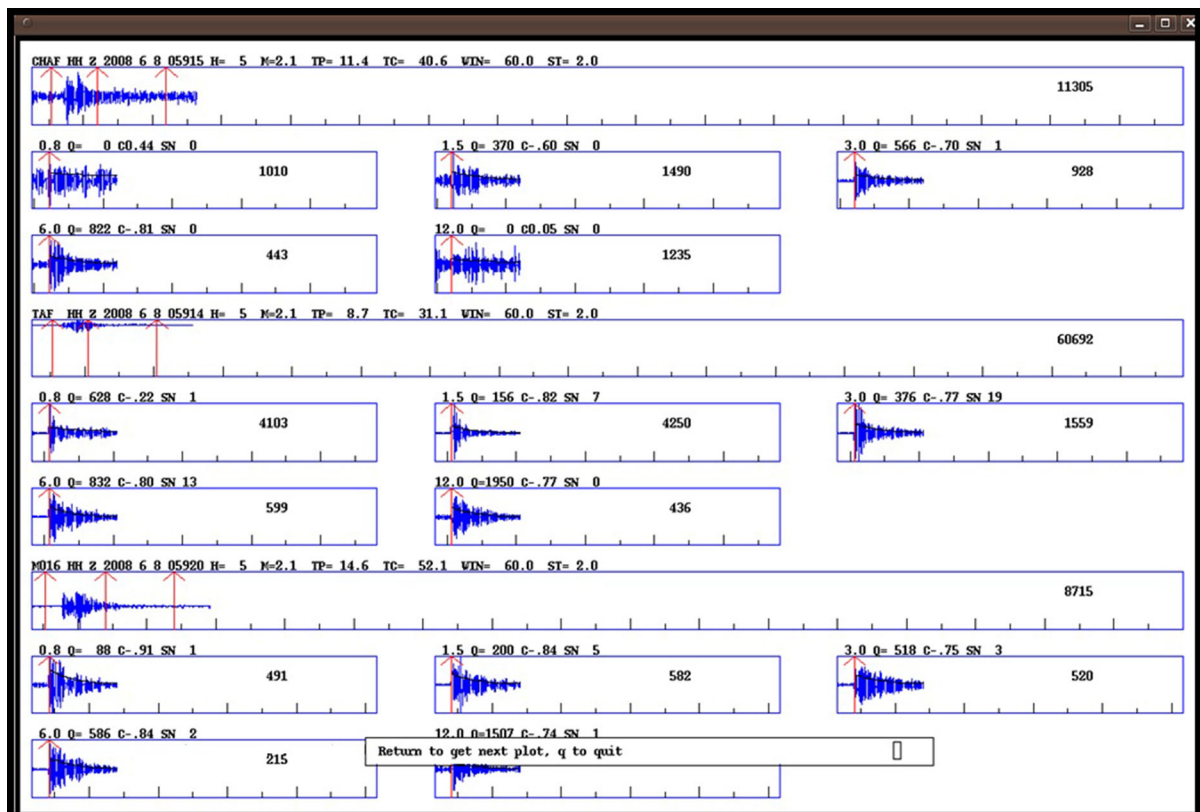


Figure 2

An example of data analysis for coda-Q estimation using the CODAQ module of Havskov and Ottemoller (2003). The seismogram from the event on 08th June, 2008 recorded at the station CHAF is band-pass filtered at five frequency bands centered at 0.75, 1.5, 3.0, 6.0 and 12.0 Hz. The coda wave portion of the 60 s duration is indicated by arrows (\uparrow). The slope of the coda envelope fitted (solid line based on Eq. 2) is used to estimate Q_c . H depth (km), M coda magnitude, TP P onset time, TC start of coda window (in sec) measured from origin time, WIN window length, ST start of coda window in terms of S travel time, $tc = 2 \times ts$, F central frequency in Hz, CO correlation coefficient, and S/N signal-to-noise ratio

5. Results and Discussion

In this study, we estimate attenuation properties of the medium using coda waves in 1.5–12 Hz in northern Morocco. For each component of motion, the average values of frequency-dependent Q_c for the whole study area are obtained by averaging the Q_c values over all the stations for each frequency (Table 4). The estimates are $Q_c = (143.75 \pm 1.09)f^{(0.864 \pm 0.006)}$, $Q_c = (140.12 \pm 1.08)f^{(0.85 \pm 0.005)}$ and $Q_c = (140.42 \pm 1.81)f^{(0.902 \pm 0.004)}$ for vertical (Z), north–south (N–S), and east–west (E–W)

component of motion, respectively. Table 5 lists the frequency-dependent power-law forms of Q_c for the three-components of motion for each lapse time (Fig. 3).

5.1. Lapse Time Dependence of Q_c

To test the lapse-time dependence of Q_c in northern Morocco, we estimate the Q_c values at four different lapse time windows of length 30, 40, 50 s and 60 s starting from 2ts. Figures 4, 5, 6 show the frequency-dependent Q_c relations for each lapse-time

Table 4

Average estimates of Q_c along with their error bars (1 standard deviation) for different frequency bands and lapse times for the three components of motion

Central frequency (Hz)	Vertical component		North–south component		East–west component	
	$Q_c \pm SD$	N	$Q_c \pm SD$	N	$Q_c \pm SD$	N
Coda window length = 30 s						
0.75	76 ± 27.77	23	86.13 ± 29.8	111	86.3 ± 36.63	10
1.5	147.38 ± 32.85	51	144.85 ± 34.89	167	164.81 ± 37.44	48
3	267.067 ± 96.65	60	265.05 ± 70.94	177	263.79 ± 99.37	48
6	506.6 ± 201.34	39	480.66 ± 162.99	155	564.44 ± 212.48	32
12	1147.6 ± 444.82	15	960.22 ± 333.15	109	1107.9 ± 464.25	15
Coda window length = 40 s						
0.75	122.48 ± 53.5	21	132.8 ± 26.46	81	101.82 ± 24.08	11
1.5	177.02 ± 30.14	55	187.33 ± 41.29	140	174.67 ± 33.77	44
3	331.94 ± 118.19	50	305.49 ± 84.04	139	310.09 ± 116.63	34
6	680.62 ± 233.46	32	664.37 ± 242.59	134	650.39 ± 271.36	31
12	1255 ± 439.2	14	1202.1 ± 451.15	100	1420.5 ± 503.6	17
Coda window length = 50 s						
0.75	141.4 ± 40.92	25	140.35 ± 34.82	71	151.57 ± 41.33	14
1.5	192.46 ± 47.03	48	212.22 ± 72.16	125	200.24 ± 52.4	37
3	367.61 ± 129.22	39	372.87 ± 122.04	133	385.1 ± 132.02	32
6	714 ± 260.38	29	688.34 ± 246.21	108	826.31 ± 269.29	26
12	1420.8 ± 245.71	13	1404.7 ± 150.04	65	1500.7 ± 111.89	9
Coda window length = 60 s						
0.75	173.89 ± 64.78	18	169.47 ± 76.05	64	136.54 ± 32.41	11
1.5	206.81 ± 51.02	42	215.64 ± 84.53	89	205.89 ± 62.58	28
3	393.05 ± 139.47	37	413.21 ± 144.08	99	449.31 ± 156.33	26
6	786.82 ± 245.22	22	724.46 ± 238.01	87	834.37 ± 239.37	19
12	1495.8 ± 50.28	8	1457.2 ± 91.39	30	1514.7 ± 79.35	6

Table 5

The power-law form of $Q_c(f) = Q_0(f)^n$ obtained for different lapse time windows for the three components of motion

Coda window length	Vertical component	East–West component	North–South component
30 s	$Q_c = (97.58 \pm 1.05)f^{(0.961 \pm 0.032)}$	$Q_c = (109.13 \pm 1.05)f^{(0.91 \pm 0.04)}$	$Q_c = (105.25 \pm 1.04)f^{(0.87 \pm 0.0245)}$
40 s	$Q_c = (139.53 \pm 1.08)f^{(0.86 \pm 0.051)}$	$Q_c = (122.49 \pm 1.07)f^{(0.95 \pm 0.046)}$	$Q_c = (146.63 \pm 1.1)f^{(0.82 \pm 0.0065)}$
50 s	$Q_c = (156.09 \pm 1.09)f^{(0.855 \pm 0.061)}$	$Q_c = (165.59 \pm 1.107)f^{(0.87 \pm 0.07)}$	$Q_c = (161.47 \pm 1.07)f^{(0.83 \pm 0.046)}$
60 s	$Q_c = (180.29 \pm 1.13)f^{(0.813 \pm 0.083)}$	$Q_c = (163.32 \pm 1.06)f^{(0.896 \pm 0.042)}$	$Q_c = (182.38 \pm 1.08)f^{(0.79 \pm 0.066)}$

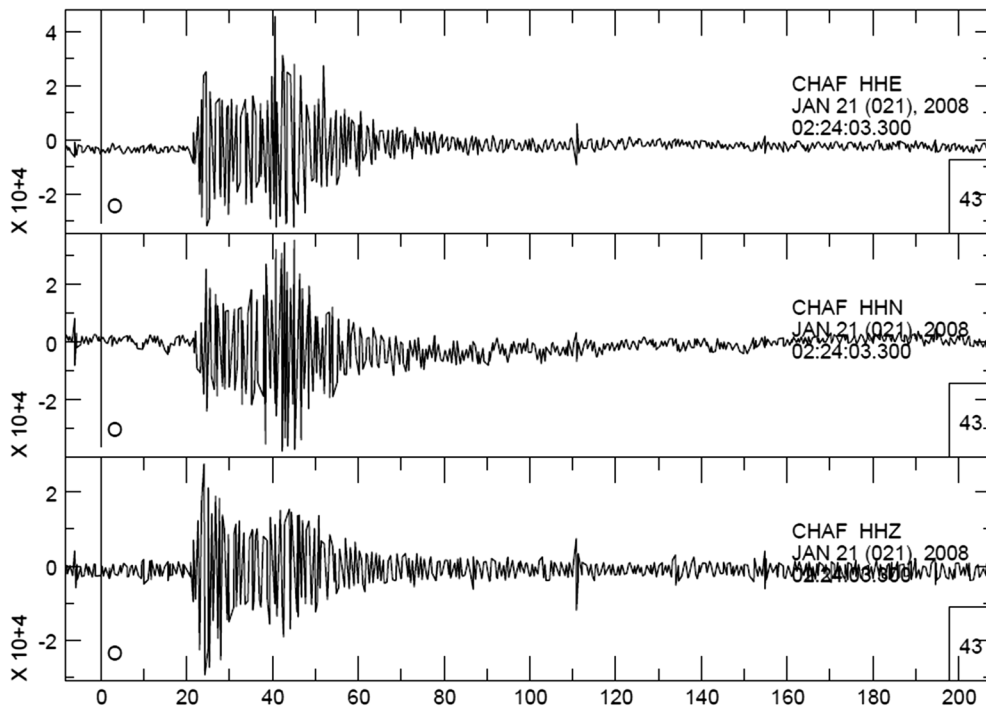


Figure 3

Typical example of three-component velocity seismograms recorded at station CHAF of the network from the event on 21 January 2008, 02:24:03:300 h. BHZ, vertical component; BHN, north–south component; BHE, east–west component. The line marked ‘O’ represents the origin time of the event

for the Z, N–S and E–W component of motion, respectively. It is shown from Figs. 4, 5, 6 that as frequency increases, the values of Q_c increase with lapse time similar to findings for several other regions (Ibanez et al. 1990; Del Pezzo and Patané 1992; Akinci et al. 1994; Gupta et al. 1998; Giampiccolo et al. 2002). Figure 7 shows the lapse time dependence of Q_0^{-1} and the exponent n , where both decrease with increase in lapse time. As an increase in large time samples the deeper part of the Earth, it is expected that both Q_0^{-1} and n decrease with increasing depth, because heterogeneity of the medium generally decreases with depth. The higher Q_0 (Q_c at 1 Hz) is expected for larger lapse times as coda is mainly dominated by the energy that has propagated in the deeper portions of the Earth with lower-attenuation zones. Thus, the observed lapse-time dependence of Q_c can be interpreted as due to increase of Q_c with depth. Depth-dependent variation in attenuation indicates the variation in level of heterogeneity with depth. The longer the analysis window, the larger is

the sample of ellipsoidal volume of the lithosphere. Thus, the variation of Q_c with lapse time can be explained by comparing different sampling volumes of the earth medium. Wennerberg (1993) showed that such a trend in Q_c can be explained by variation in intrinsic or scattering attenuation in the expanding volume of earth medium sampled by coda waves, assuming multiple scattering of S-waves. Our method is based on the single back-scattering of seismic S-waves. For evaluating the relative contributions of intrinsic and scattering attenuations to the total attenuation, we need a multiple scattering model of coda wave generation, however. We plan to do such analysis with a widely used multiple lapse time window analysis (MLTWA) method, as a scope of future study (Masahiro 1992; Tuvè et al. 2006; Woodgold 1994).

We cannot attribute the lapse time dependence of Q_c entirely to the effect of depth, however. The lapse-time dependence of Q_c is also expected in cases where (1) the distribution of scatterers is

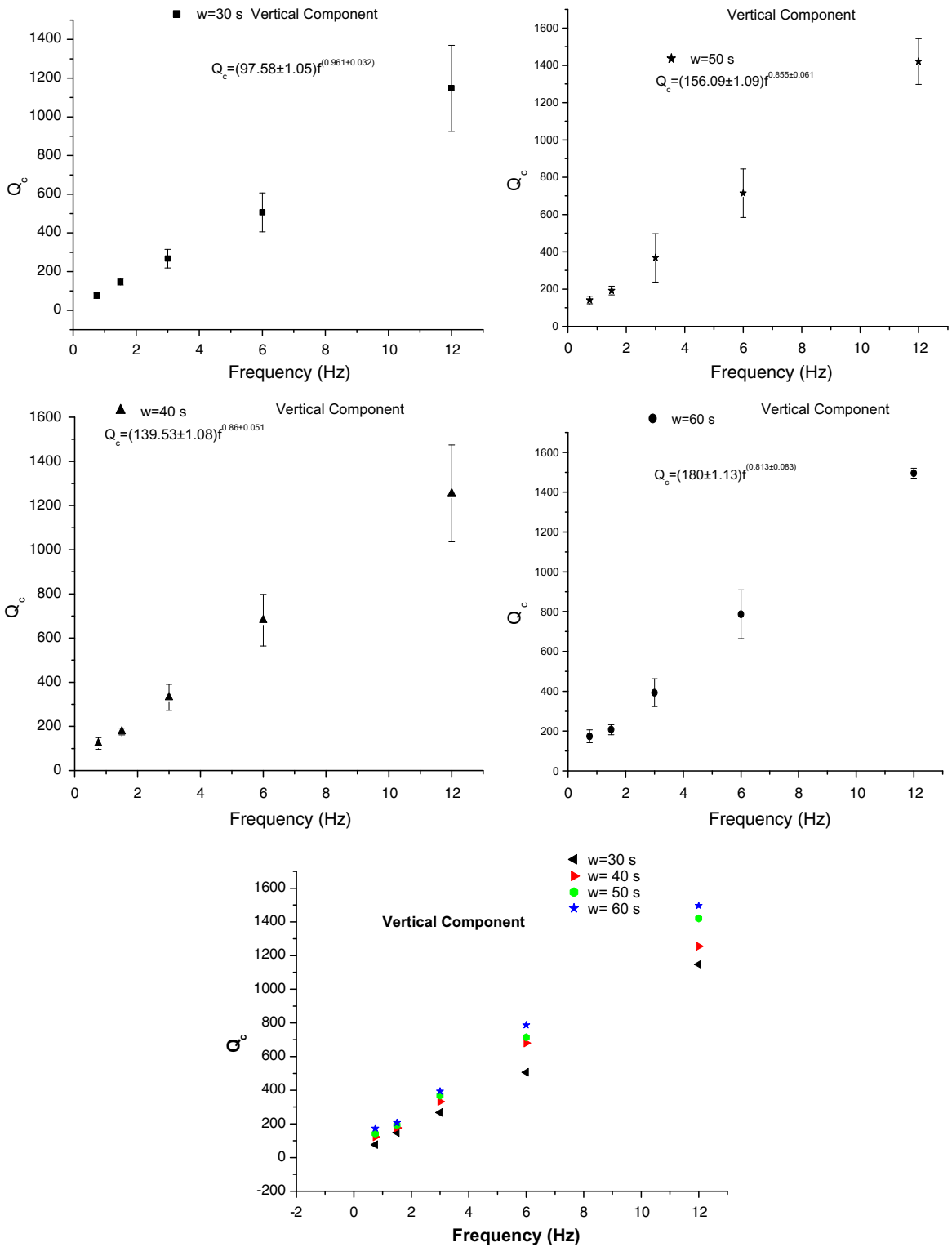


Figure 4

Lapse time dependence of $Q_c(f)$ for the vertical (Z) component of motion, as shown in the uppermost four plots. They are again shown in one plot for comparison (bottom figure)

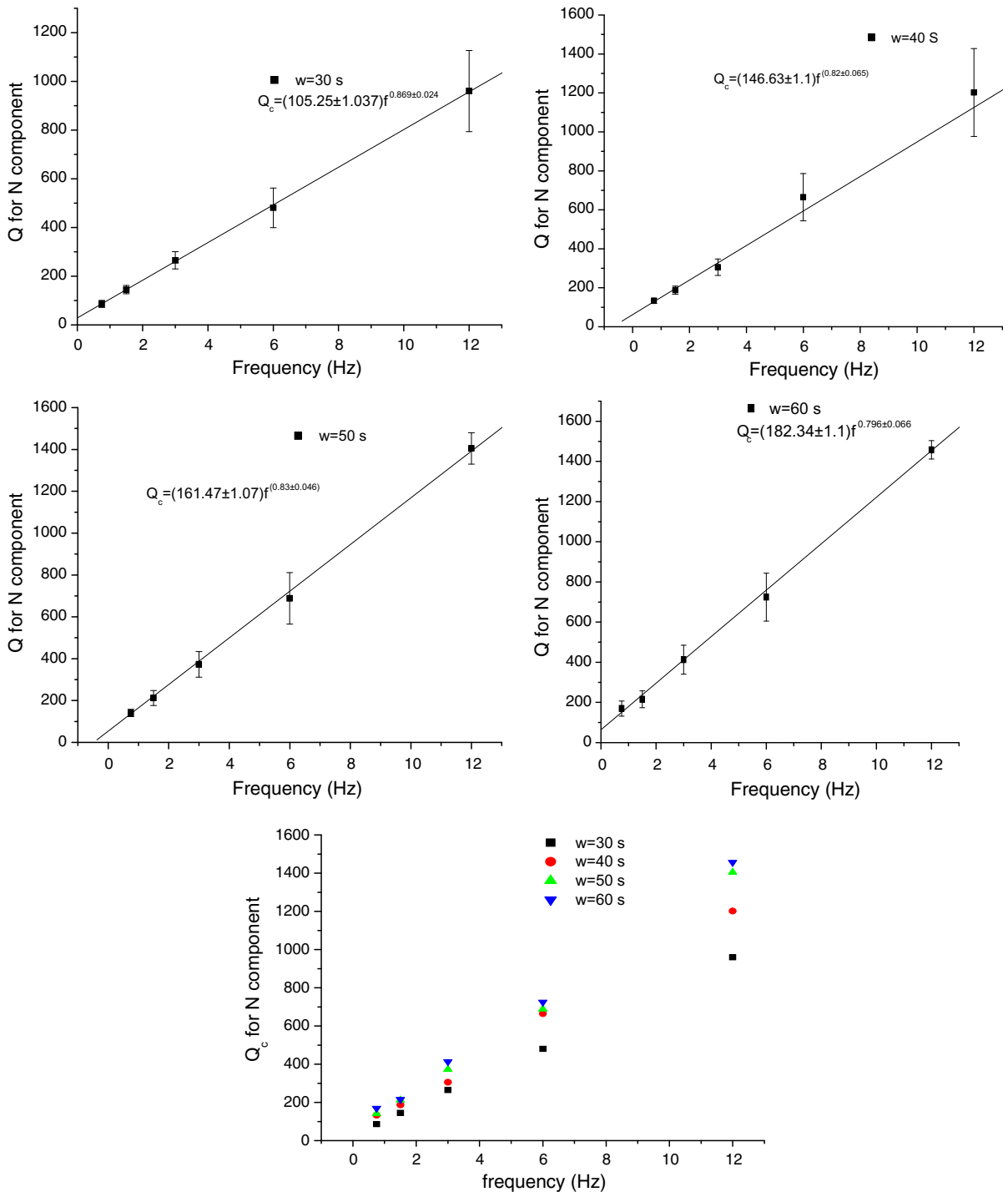


Figure 5
Same as Fig. 4, but for the N-S component of the motion

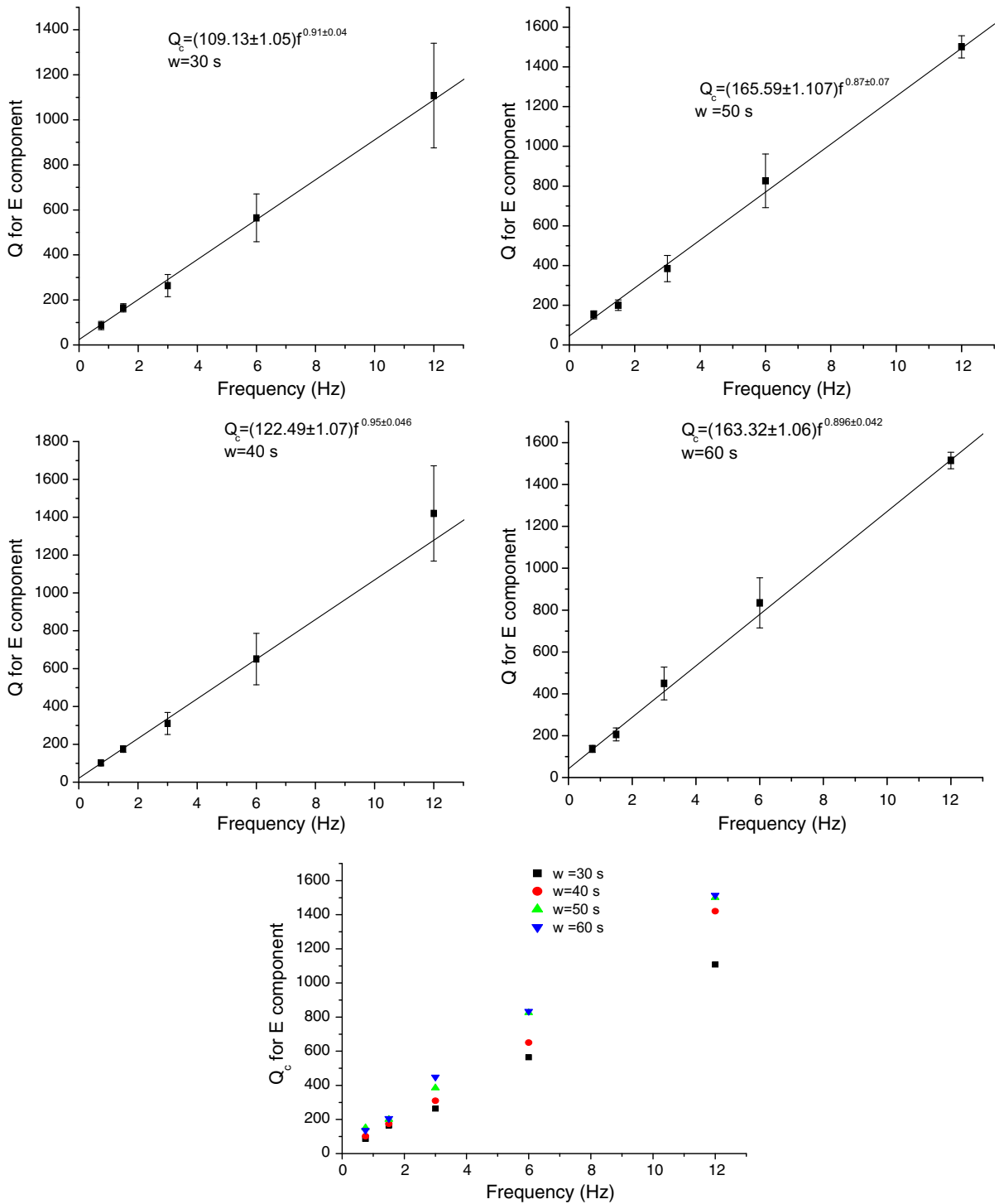


Figure 6
Same as Fig. 4, but for the E-W component of the motion

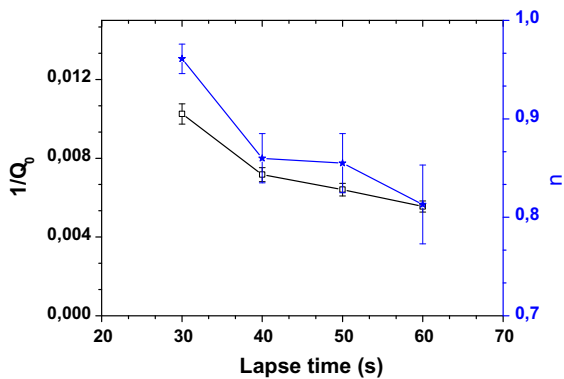


Figure 7

Comparison of average values of $1/Q_0$ and n with lapse time for vertical component of motion

heterogeneous, with more scatterers being present at shallower depths, (2) the intrinsic Q of the medium is not constant, or (3) multiple scattering occurs in the late coda. For local events with a short lapse time window (less than 100 s), the effect of multiple scattering is not significant (Kopnischev 1977; Gao et al. 1983). For regional events with long lapse times (greater than mean free time), however, a contribution of multiple scattering to the lapse-time dependence of Q_c cannot be neglected (Padhy and Subhadra 2010). For example, Del Pezzo et al. (1991) have shown for the Etna volcano data that the single back-scattering model cannot be used to explain the lapse-time dependence of coda waves. The length of lapse-time window for multiple scattering to become significant depends on the scale length of the heterogeneities of the medium. In this study, however, the lengths of lapse-time window are less than 100 s, so the use of single scattering model is acceptable for the study area.

The average Q_c relations for the study area for the vertical component of motion are $Q_c(f) = (97.6 \pm 1.05)f^{(0.96 \pm 0.03)}$, $Q_c(f) = (139.5 \pm 1.08)f^{(0.86 \pm 0.05)}$, $Q_c(f) = (156.1 \pm 1.09)f^{(0.86 \pm 0.06)}$ and $Q_c(f) = (180.3 \pm 1.13)f^{(0.81 \pm 0.08)}$ for lapse-time windows of 30, 40, 50 and 60 s, respectively. The frequency dependence of Q_c is related to scale length of heterogeneities of the medium. The strong frequency dependence could be related to a high degree of heterogeneity of the medium (Mayeda et al. 1992).

The Q_c values are considered to represent an average over the ellipsoid volume sampled by coda

waves for a given lapse-time (Pulli 1984). For a given average lapse-time t , the surface projection of such ellipsoid with foci at the source and receiver is defined by

$$\frac{x^2}{(vt/2)^2} + \frac{y^2}{(vt/2)^2 - (r/2)^2} = 1, \quad (3)$$

with the semi-major axes $a = vt/2$ and semi-minor axes $b = \sqrt{(vt/2)^2 - (r/2)^2}$, v is S-wave velocity, r is the source-receiver distance, and x and y are the surface coordinates (Pulli 1984). The average lapse time t is taken as $t = t_{\text{start}} + \frac{W}{2}$, where t_{start} is the starting time of the coda window and W is the coda window length. The maximum depth of sampling that is related to semi-major axes is about 105 km assuming an average S-wave speed of 3.5 km/s in the medium. Our analysis assumes a uniform velocity model of the whole medium beneath the region, although in reality velocity varies with depth. Thus, we think that our Q_c estimates represent the average attenuation properties of the whole crust and part of the upper mantle beneath northern Morocco.

For an average S-wave velocity of 3.5 km/s, the length of the larger semi-major axis is approximately 53 and 105 km for 30 and 60 s lapse time, respectively, which clearly shows how multiple scattering, which is expected to occur at large lapse-times, reduces the volume sampled by coda waves, although the effect of multiple scattering seems to be minimum in this case. Our findings are similar to those of Ibanez et al. (1990) who compared the volume sampled by the scattered waves for a fixed lapse time (70 s) for seismic sources located at different depths. They observed that for events at greater depths, the larger semi-major axis is about 150 km long, decreasing to about 110 for shallow earthquakes in Granada, southern Spain. Thus, the effects of multiple scattering shorten the sampling volume of the medium.

5.2. Variation of Q_c for the Three Components of Motion

The average values of Q_c for the three components of motion are plotted in Fig. 8. The $Q_c(f)$ values for the three components of motion are similar at all frequencies analyzed, which is expected because of

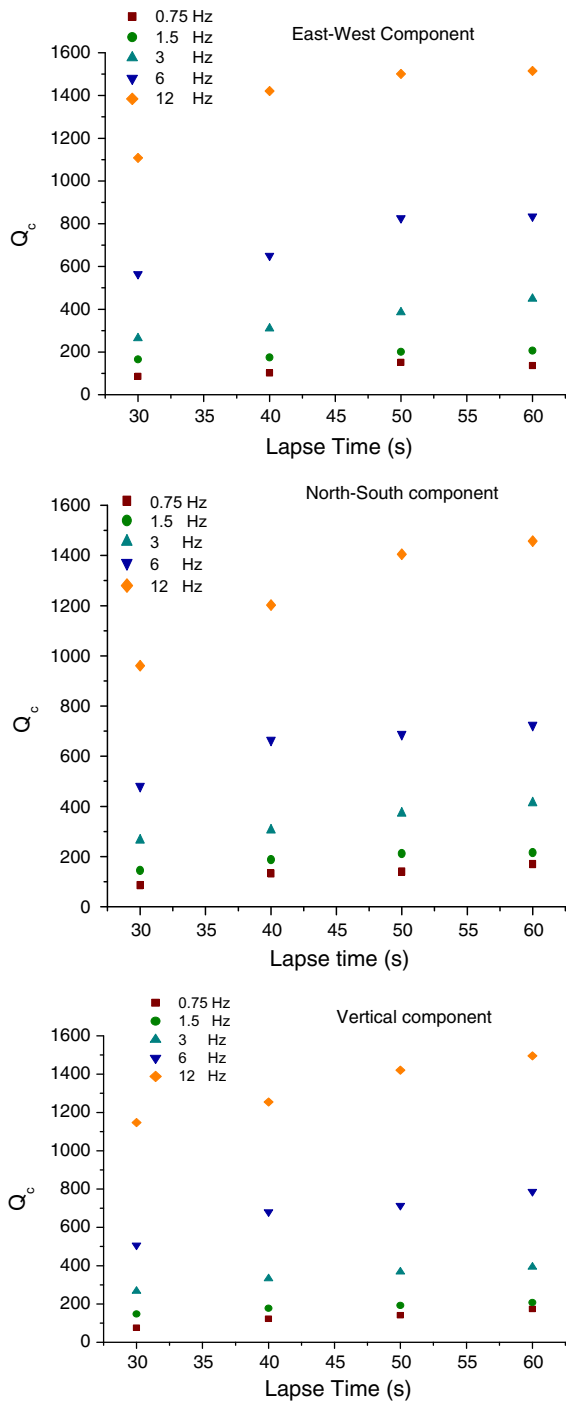


Figure 8

Plots summarizing the lapse time dependence of $Q_c(f)$ for all the three-components of motion

averaging over a larger volume of the medium sampled by coda waves (Fig. 8 and Table 5). It might also be possible that different radiation patterns

may give rise to differential energy decay pattern in three components of motion, but their effect is negligible for coda waves at high frequencies. Sato (1984) has shown that in case of single scattering, the directional partition of energy in S-coda depends on the focal mechanism and hence on radiation pattern for a point source dislocation. These differences in source radiation pattern are averaged out in later coda arrivals, which make the Q_c values insensitive to the component of ground motion. A similar estimate of Q_c , that is independent of the component of ground motion, is found for volcanic micro-earthquakes at CampiFlegrei (Del Pezzo et al. 1985).

5.3. Comparison with Other Results

In general, the estimates of Q_c can be affected by differences in parameters such as coda window length and coda onset time, distance and depth of events used, frequency range, use of body or surface waves, and the type of model used to determine Q_c (Table 6).

Here, we compared Q_c values for different areas obtained from coda waves for similar coda onset time and lapse-time that sample approximately similar volumes of the medium sampled (Fig. 9). To minimize the influence of the use of different model parameters on Q_c measurements, we compared our results with others using the similar method. The comparison shows that the study area is seismically (1) more active than New England, central and northeastern USA (Phillips and Aki 1986), (2) less active than east central Iran, Yunnan in China, Washington State, Parkfield in

Table 6

Worldwide Q studies done in active and stable areas

Places	Q_0	n	Source
<i>Active regions</i>			
Yao'an area in Yunnan Province	49	0.95	Li et al. (2004)
Zagros continental collision zone S.Iran	99	0.84	Rahimi and Hamzehloo (2008)
Granada zone (Southern Spain)	155	0.89	Ibanez et al. (1990)
Washington State	63	0.97	Havskov et al. (1989)
<i>Stable regions</i>			
New England	460	0.45	Pulli (1984)
Iberian Peninsula	600	0.45	Pujades et al. (1990)

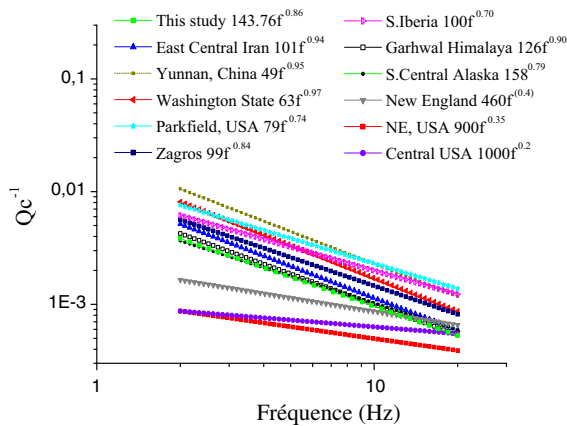


Figure 9

Comparison of the coda- Q_c values of the Northern Morocco region with those of other regions of the world (Ma'hood and Hamzehloo 2009; Singh and Hermann 1983)

USA, Zagros, and southern Iberia, and (3) similar to Garhwal Himalaya in India and south central Alaska. Such a regional variation in Q_c can be interpreted in terms of (1) vertical and lateral variation in structural heterogeneities among the regions (Aki 1969; Steck et al. 1989; Fehler et al. 1992), (2) velocity contrast in a layered structure (Hoshiya 1997; Margerin et al. 1998), and (3) near-surface effects, focusing and defocusing of seismic waves (Frankel and Wennerberg 1987).

Regions with active tectonics are generally associated with low Q_0 (less than 200) values, and vice versa such as the Yunnan Province in China ($Q_0 = 49$ and $n = 0.95$, Li et al. 2004), Zagros continental collision zone in southwestern Iran ($Q_0 = 99$ and $n = 0.84$, Rahimi and Hamzehloo 2008), Granada zone (southern Spain) ($Q_0 = 155$ and $n = 0.89$, Ibanez et al. 1990) and the state of Washington ($Q_0 = 63$ and $n = 0.97$, Havskov et al. 1989). On the contrary, stable regions are characterized by relatively high values of Q_0 (more than 200), such as New England ($Q_0 = 460$, $n = 0.45$; Pulli 1984), N. Iberia ($Q_0 = 600$, $n = 0.45$; Pujades 1991). The value of the exponent n increases with the intensity of tectonic activity and is more than 1.0 for tectonically active regions.

6. Conclusions

In this work, the attenuation proprieties of high-frequency (> 1 Hz) coda waves are studied for

northern Morocco. The average frequency-dependent Q_c values for three components of ground motion are found to be similar, suggesting the average property of the medium sampled by coda waves over a large sampling volume. The estimates of Q_c and their frequency dependences are found to be similar to those for active regions of the world like Garhwal Himalaya and south central Alaska. Lapse-time dependence of Q_c could be related to the depth-dependent variation in attenuation and hence in level of heterogeneity of the medium. Strong frequency dependence suggests high degree of heterogeneity of the medium associated with complex subduction structure of the medium. On comparing the estimated Q_c values with other regions indicates that the northern Morocco is seismically active characterised by low values of Q_c and hence by relatively high attenuation. These results will be useful in characterizing the path effect that is necessary for ground motion modelling in the region.

Acknowledgements

We sincerely thank the anonymous reviewers and the Editor Professor Ruben Tatevossian for their constructive comments that improved the quality of the paper. We thank the Scientific Institute of Rabat/Morocco for providing the data used in this study. Some of the figures were produced using the Generic Mapping Tools software (Wessel and Smith 1998).

REFERENCES

- Aki, K. (1969). Analysis of the seismic coda of local earthquakes: source, attenuation and scattering effects. *Journal of Geophysical Research*, 74(2), 615–631.
- Aki, K., & Chouet, B. (1975). Origin of coda waves: source, attenuation, and scattering effects. *Journal of Geophysical Research*, 80(23), 3322–3342.
- Akinci, A., Taktak, A. G., & Ergintav, S. (1994). Attenuation of coda waves in Western Anatolia. *Physics of the Earth and Planetary Interiors*, 87(1–2), 155–165.
- Badawy, A., & Morsy, M. A. (2012). Seismic Wave Attenuation in the Greater Cairo Region. *Egypt. Pure and applied geophysics*, 169(9), 1589–1600.
- Biescas, B., Rivera, Z., & Zapata, J. A. (2007). Seismic attenuation of coda waves in the eastern region of Cuba. *Tectonophysics*, 429(1), 99–109.

- Boulanouar, A., El Moudnib, L., Ford, S., Harnafi, M., Villasenor, A., Gallart, J., et al. (2016). Coda wave attenuation tomography in Northern Morocco. *Journal of Materials and Environmental Science*, 7(8), 2880–2885.
- Boulanouar, A., El Moudnib, L., Harnafi, M., Cherkaoui, T. E., Rahmouni, A., Boukalouch, M., et al. (2013). Spatial variation of coda wave attenuation using aftershocks of the Al Hoceima earthquake of 24 February, 2004. *Morocco. Natural Science*, 5(08), 72.
- Cherkaoui, T. E., & El Hassani, A. (2012). Seismicity and seismic hazard in Morocco: 1901–2010. *Bulletin de l'Institut Scientifique, Rabat, Section Sciences de la Terre*, 34, 45–55.
- Cherkaoui, T. E., Hatzfeld, D., Jebli, H., Medina, F., & Caillot, V. (1990). Etude microsismique de la region d'Al Hoceima. *Bulletin de l'Institut Scientifique*, 14, 25–34.
- Del Pezzo, E., De Martino, S., De Miguel, F., Ibanez, J., & Sorgente, A. (1991). Characteristics of the seismic attenuation in two tectonically active zones of Southern Europe. *Pure and Applied Geophysics*, 135(1), 91–106.
- Del Pezzo, E., De Natale, G., Scarcella, G., & Zollo, A. (1985). Qc of three component seismograms of volcanic microearthquakes at Campi Flegrei volcanic area—southern Italy. *Pure and Applied Geophysics*, 123(5), 683–696.
- Del Pezzo, E., & Patané, D. (1992). Coda Q dependence on time, frequency and coda duration interval at Mt. Etna, Sicily. In E. Del Pezzo & D. Patané (Eds.), *Volcanic seismology* (pp. 109–119). Heidelberg: Springer.
- El Moudnib, L., Villaseñor, A., Harnafi, M., Gallart, J., Pazos, A., Serrano, L., et al. (2015). Crustal structure of the Betic-Rif system, western Mediterranean, from local earthquake tomography. *Tectonophysics*, 643, 94–105.
- Fehler, M., Hoshihara, M., Sato, H., & Obara, K. (1992). Separation of scattering and intrinsic attenuation for the Kanto-Tokai region, Japan, using measurements of S-wave energy versus hypocentral distance. *Geophysical Journal International*, 108(3), 787–800.
- Frankel, A., & Wennerberg, L. (1987). Energy-flux model of seismic coda: separation of scattering and intrinsic attenuation. *Bulletin of the Seismological Society of America*, 77(4), 1223–1251.
- Gao, L. S., Lee, L. C., Biswas, N. N., & Aki, K. (1983). Comparison of the effects between single and multiple scattering on coda waves for local earthquakes. *Bulletin of the Seismological Society of America*, 73(2), 377–389.
- Giampiccolo, E., Tusa, G., Langer, H., & Gresta, S. (2002). Attenuation in southeastern Sicily (Italy) by applying different coda methods. *Journal of Seismology*, 6(4), 487–501.
- Gupta, S. C., Teotia, S. S., Rai, S. S., & Gautam, N. (1998). Coda Q estimates in the Koyna region, India. *Pure and Applied Geophysics*, 153(2–4), 713.
- Havskov, J., Malone, S., McClurg, D., & Crosson, R. (1989). Coda Q for the state of Washington. *Bulletin of the Seismological Society of America*, 79(4), 1024–1038.
- Havskov, J., Ottemoller, L. (2003). SEISAN: the earthquake analysis software for windows, Solaris, Linux, and Mac OSX Version 8.0. <http://www.geo.uib.no/Seismologi/SOFTWARE/>. Accessed 4 March 2014.
- Hoshihara, M. (1997). Seismic coda wave envelope in depth-dependent S wave velocity structure. *Physics of the Earth and Planetary Interiors*, 104(1–3), 15–22.
- Ibanez, J. M., Del Pezzo, E., De Miguel, F., Herraiz, M., Alguacil, G., & Morales, J. (1990). Depth-dependent seismic attenuation in the Granada zone (Southern Spain). *Bulletin of the Seismological Society of America*, 80(5), 1232–1244.
- Inmaculada, S., Dapeng, Z., José, M., & Federico, T. (2003). Seismic tomography from local crustal earthquakes beneath eastern Rif Mountains of Morocco. *Tectonophysics*. [https://doi.org/10.1016/S0040-1951\(03\)00100-8](https://doi.org/10.1016/S0040-1951(03)00100-8).
- Khattach, D., Houari, M. R., Corchete, V., Chourak, M., El Gout, R., & Ghazala, H. (2013). Main crustal discontinuities of Morocco derived from gravity data. *Journal of Geodynamics*, 68, 37–48.
- Kopnichev, Y. (1977). The role of multiple scattering in the formation of a seismogram's tail. *Izvestiya, Earth Phys.*, 13, 394–398.
- Kumar, N., Parvez, I. A., & Virk, H. S. (2005). Estimation of coda wave attenuation for NW Himalayan region using local earthquakes. *Physics of the Earth and Planetary Interiors*, 151(3), 243–258.
- Lee, W. S. (1999). Q estimates using the coda waves in the Kyeongsang Basin. Thesis for an M.S. Degree. Department of Geological Science: Graduate School Seoul National University.
- Li, B. J., Qin, J. Z., Qian, X. D., & Ye, J. Q. (2004). The coda attenuation of the Yao'an area in Yunnan Province. *Acta Seismologica Sinica*, 17(1), 47–53.
- Ma'hood, M., & Hamzehloo, H. (2009). Estimation of coda wave attenuation in East Central Iran. *Journal of Seismology*, 13(1), 125–139.
- Mamdouh, A. M., El Hady, S., Mahmoud, S. M., & Awad, E. A. M. (2013). Lateral variations of coda Q and attenuation of seismic waves in the Gulf of Suez. *Egypt. Arabian Journal of Geosciences*, 6(1), 1–11.
- Margerin, L., Campillo, M., & Tiggelen, B. (1998). Radiative transfer and diffusion of waves in a layered medium: new insight into coda Q. *Geophysical Journal International*, 134(2), 596–612.
- Masahiro, K. (1992). Dependence of coda Q on frequency and lapse time. *Journal of Physics of the Earth*, 40(2), 421–445.
- Mayeda, K., Koyanagi, S., Hoshihara, M., Aki, K., & Zeng, Y. (1992). A comparative study of scattering, intrinsic, and coda Q—1 for Hawaii, Long Valley, and central California between 1.5 and 15.0 Hz. *Journal of Geophysical Research: Solid Earth*, 97(B5), 6643–6659.
- Medina, F., & El Alami, S. O. (2006). Focal mechanisms and state of stress in the Al Hoceima area (Central Rif, Morocco). *Bulletin de l'Institut Scientifique, Rabat*, 28, 19–30.
- Mukhopadhyay, S., & Tyagi, C. (2007). Lapse time and frequency-dependent attenuation characteristics of coda waves in the Northwestern Himalayas. *Journal of Seismology*, 11(2), 149–158.
- Padhy, S., & Subhadra, N. (2010). Attenuation of high-frequency seismic waves in northeast India. *Geophysical Journal International*, 181(1), 453–467.
- Parvez, I. A., Sutar, A. K., Mridula, M., Mishra, S. K., & Rai, S. S. (2008). Coda Q estimates in the Andaman Islands using local earthquakes. *Pure and Applied Geophysics*, 165(9), 1861–1878.
- Phillips, W. S., & Aki, K. (1986). Site amplification of coda waves from local earthquakes in central California. *Bulletin of the Seismological Society of America*, 76(3), 627–648.
- Pujades, L. G., Canas, J. A., Egozcue, J. J., Puigvi, M. A., Gallart, J., Lana, X., et al. (1990). Coda-Q distribution in the Iberian Peninsula. *Geophysical Journal International*, 100(2), 285–301.
- Pullin, J. J. (1984). Attenuation of coda waves in New England. *Bulletin of the Seismological Society of America*, 74(4), 1149–1166.

- Rahimi, H., & Hamzehloo, H. (2008). Lapse time and frequency-dependent attenuation of coda waves in the Zagros continental collision zone in Southwestern Iran. *Journal of Geophysics and Engineering*, 5(2), 173.
- Rautian, T. G., & Khalturin, V. I. (1978). The use of the coda for determination of the earthquake source spectrum. *Bulletin of the Seismological Society of America*, 68(4), 923–948.
- Sato, H., Fehler, M. C., & Maeda, T. (2012). *Seismic wave propagation and scattering in the heterogeneous earth* (Vol. 496). Berlin: Springer.
- Singh, D. D., Govoni, A., & Bragato, P. L. (2001). Coda Qc attenuation and source parameter analysis in Friuli (NE Italy) and its vicinity. *Pure and Applied Geophysics*, 158(9–10), 1737–1761.
- Singh, S., & Herrmann, R. B. (1983). Regionalization of crustal coda Q in the continental United States. *Journal of Geophysical Research: Solid Earth*, 88(B1), 527–538.
- Steck, L. K., Prothero, W. A., & Scheimer, J. (1989). Site-dependent Coda Q at mono craters, California. *Bulletin of the Seismological Society of America*, 79(5), 1559–1574.
- Timoulali, Y., Hahou, Y., Jabour, N., Merrouch, R., & El Kharrim, A. (2014). Main features of the deep structure by local earthquake tomography and active tectonics: case of Rif Mountain (Morocco) and Betic Cordillera (Spain). *Journal of Seismology*, 18(2), 221–234.
- Tuvè, T., Bianco, F., Ibáñez, J., Patanè, D., Del Pezzo, E., & Bottari, A. (2006). Attenuation study in the Straits of Messina area (southern Italy). *Tectonophysics*, 421(3), 173–185.
- Wennerberg, L. (1993). Multiple-scattering interpretations of coda-Q measurements. *Bulletin of the Seismological Society of America*, 83(1), 279–290.
- Wessel, P., & Smith, W. H. (1998). New, improved version of generic mapping tools released. *Eos, Transactions American Geophysical Union*, 79(47), 579.
- Woodgold, C. R. D. (1994). Coda Q in the Charlevoix, Quebec, region: lapse-time dependence and spatial and temporal comparisons. *Bulletin of the Seismological Society of America*, 84(4), 1123–1131.

(Received August 5, 2017, revised November 13, 2017, accepted November 16, 2017, Published online November 28, 2017)